Response Characteristics of Water Hydraulic Proportional Control Valves*

YOSHIDA Futoshi

Abstract

Water hydraulic proportional control valves using "tap water" as the working fluid are suitable for systems that require high levels of environmental friendliness and safety as they use "tap water" as the working fluid. There is a high level of expectation for applications in the fields of food processing machinery and semiconductor manufacturing equipment in particular. In the previous report, the authors defined the transfer functions of three components of the water hydraulic proportional control valve, namely the compensation circuit, the solenoid, and the pilot valve, and examined the effects of design parameters on valve performance using experimental and analytical methods. These water hydraulic proportional control valves use tap water, which has poor lubricating properties, as the working fluid, and the hydrostatic bearings and damping orifices that make up their mechanical features function to prevent friction and wear in the spool, and stable operation of the spool itself. The structure of the hydrostatic bearings also consist of a meter-in circuit that is effective for spool operation response, while the damping orifices consist of a meter-out circuit that is effective for damping characteristics of the spool; their functions are used as required depending on the purpose of the valve. This report focuses on the open loop transfer function represented by the solenoid and the pilot valve sections that have a major impact on the characteristics of the entire valve, examines the effect of hydrostatic bearing and damping orifice geometric parameters, and verifies analytically the step response characteristics that these parameters have on the entire valve.

1 Introduction

Water hydraulic proportional control valves are suitable for systems that require high levels of hygiene and safety as they use "tap water" as the working fluid. Their application scope is vast, including food, beverage, semiconductors, medicine, pharmaceuticals, cosmetics, chemicals, natural energy, and underwater work equipment.

Realization of systems with high levels of hygiene and detergency is anticipated, especially with automation of meat/seafood processing, which has conventionally been manually performed.

In the previous report, I defined the transfer functions of three components of this valve, namely the compensation circuit, the solenoid, and the pilot valve, and examined the effects of design parameters on valve performance by using experimental and analytical methods for each element [1)-5)]. This valve uses tap water, which has poor lubricating properties, as the working fluid. In this structure, the hydrostatic bearings support both ends of the spool to prevent wear and friction, and the fluid that comes through the hydrostatic bearings is guided to the pressure chambers on both ends of the spool, generating damping force to stabilize the spool operation. Due to their positions in response to spool operation, the structure of the hydrostatic bearing orifices consists of a meter-in circuit, and the structure of the damping orifices consists of a meter-out circuit. A meter-in circuit is effective for spool operation response, while the meter-out circuit is effective for damping characteristics of the spool; their functions are used as required depending on the purpose. While these dimensions must be set at the optimal values to stabilize the valve, no sufficient theoretical study had been conducted so they were empirically determined.

This report focuses on the open loop transfer functions represented by the solenoid and the pilot valve sections that have a major impact on the characteristics of the entire valve, examines the effect of the geometric parameters, and verifies the characteristics of the entire valve from the perspective of response characteristics. Specifically, the dimension difference between the equivalent throttle diameter D'_b of the hydrostatic bearing orifices and damping orifices diameter D_n is defined as $C_r = D_n / D'_b$ to analytically study: (1) the impact of C_r changes on T_L, which is the time constant of the first-order lag system for the pilot valve, (2) impact of C_r changes on ζ, which is the damping coefficient of the second-order lag system including solenoid and pilot valve sections, and (3) impact of C_r on the step response of the open loop transfer function, including the compensation circuit of the entire valve [6)].

2 | Overview of Water Hydraulic Proportional Control Valves

The structural characteristics and control method of water hydraulic proportional control valves are as follows:

2.1 Structure

Fig. 1 shows the structure of water hydraulic proportional valves. Table 1 shows the main specifications. Since they use tap water with low viscosity as the working fluid, it is difficult to form a water film in the gap of the sliding part. Due to this, hydrostatic bearings are used to support both ends of the spool of this valve. The spool displaces without coming in contact with the sleeve with the aim of reducing the wear and friction from sliding.

There are damping orifices between the pressure chambers on both ends of the spool and the return line. This structure creates damping force for the spool operations, thus stabilizing the valve operations.

The spool is oriented with the solenoid's thrust and spring force. While general solenoid valves are structured so that both ends of the spool are supported by a solenoid and a compression spring, this valve uses a tension spring. Using a tension spring creates a free edge on one side of the spool, so hydrostatic bearings can more efficiently function in response to the reduction of moment and lateral force.
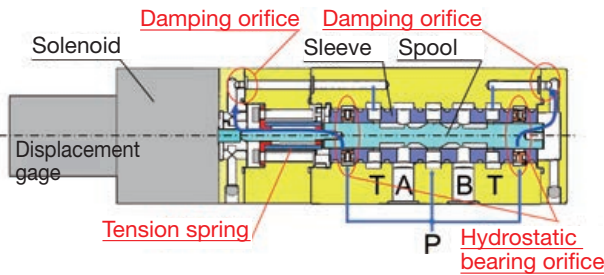

Fig. 1 Structure

Table 1 Main specifications

Item	Specifications
Rated flow	20L/min
Used pressure range	3.5 - 14MPa
Used temperature range	2 - 50°C
Working fluid	Tap water

2.2 Functions of the Hydrostatic Bearing Orifices and Damping Orifices

Fig. 2 shows the schematic positional relation of the spool, hydrostatic bearing orifices, and damping orifices. The function of the hydrostatic bearing orifices is to support the spool within the sleeve without coming in contact with it in order to prevent wear/friction, so the design dimensions are determined by the load capacity to support the spool [1]. The fluid that passes the hydrostatic bearing orifices is guided to the pressure chamber on the spool edge. When this passes the damping orifices, the damping force is created. Therefore, the design dimensions of the damping orifices depend on the design dimensions of the hydrostatic bearing orifices and are not determined in a definite manner.

As the hydrostatic bearing orifices' function to support the spool without coming in contact with it and the positional relation with the spool suggests, the hydrostatic bearing orifices function as the meter-in circuit against the spool operation and are effective against the fast response of the spool operation. On the other hand, the damping orifices function as the meter-out circuit against the spool operation and have the damping effect on the spool operation. Whether the meter-in function or meter-out function works more effectively against spool operation is determined by the relative relation of the two orifices. In other words, if the hydrostatic bearing orifices are relatively smaller than the damping orifices, the meter-in effect would be stronger. On the other hand, if the damping orifices are relatively and sufficiently larger than the hydrostatic bearing orifices, the meter-out effect would be stronger. If they are the same, it is assumed that the meter-in and meter-out effects are combined to effect the spool operation.

In general, water viscosity is extremely small at approximately 1/30 of oil, so it is assumed that the orifice diameter must be extremely small in order to create sufficient damping force. From a practical perspective, reduction of the orifice diameter creates a concern for contamination. Due to this, hardly any quantitative studies on its effect have been performed. With regard to this aspect, this report targets these valves and studies the frictional coefficient, which is required to calculate the damping force of the damping orifices, by comparing with oil.

First, the relationship between the orifice diameter D and the Reynolds number R_e is calculated by using orifice dimensions and the actual measurement value of the flow volume [2]. For example, if the orifice diameter is $\varphi 0.6$, the water's Reynolds number is approximately 9,000, creating a turbulent flow. On the other hand, oil's Reynolds number is approximately 300, creating a laminar flow. This indicates that the flow conditions differ between water and oil, despite the same orifice diameter. Next, Fig. 3 shows the relationship between Reynolds number R_e and frictional coefficient λ. Since oil creates a laminar flow, $\lambda = 64/R_e$ is applied based on the Hagen-Poiseuille equation, resulting in the frictional coefficient of $\lambda_{Oil} = 0.22$. On the other hand, due to the fact water creates a turbulent flow, $\lambda = 0.3164/R_e^{0.25}$ is applied based on the Blasius equation, resulting in the frictional coefficient of $\lambda_{Water} = 0.033$. Based on this, we know that the frictional coefficient of water is approximately 1/6 of that of oil.

Based on the above results, Fig. 4 shows the comparison of the damping forces between water and oil, which are calculated by using the general orifice diameter. This result shows that the orifice diameter for water needs to be approximately half of that for oil in order for water to gain the same level of damping force as oil. From the mass
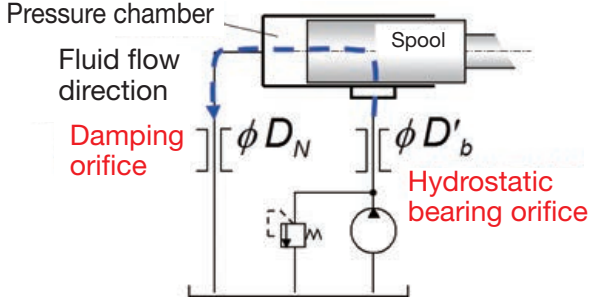
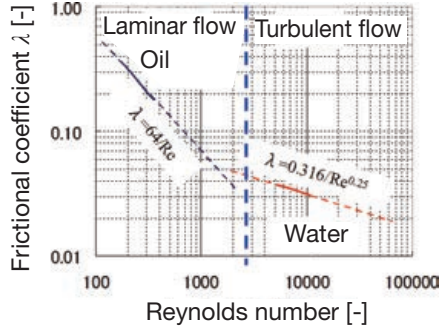**Fig. 2** Positions of hydrostatic bearing orifices and damping orifices in relation to the spool

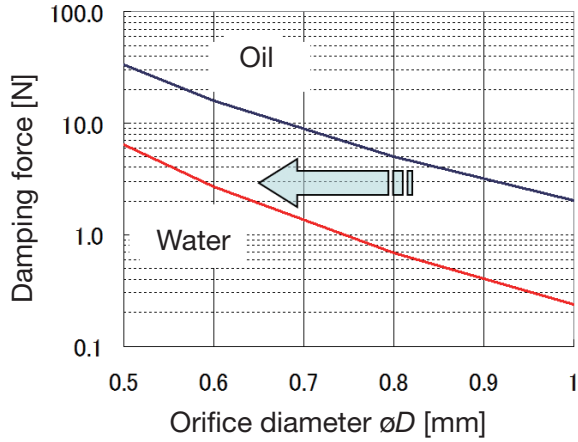**Fig. 3** Relationship between Reynolds number R_e and Frictional coefficient λ

Fig. 4 Relationship between orifice diameter and damping force

production perspective, reducing the orifice diameter makes improvement of the hole drilling precision and contamination measures even more difficult. Due to this, in order to gain damping force in water pressure systems, reducing the damping orifice diameter is not sufficient. It is appropriate to use circuit configurations by integrating meter-in and meter-out effects, such as those mentioned in this report.

2.3 Control Method

Fig. 5 shows the block diagram for the system within the valve. This valve can be divided into the elements of the compensation circuit, solenoid, and valve. The transfer function for each is represented by $C(s)$, $S(s)$, and $P(s)$. The spool displacement is detected by the displacement

gauge of the operation transformer, and the displacement is provided as feedback; the PI control compensation circuit operates the valve control.
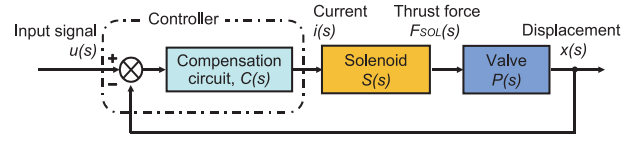

Fig. 5 Block diagram

3 Transfer Function

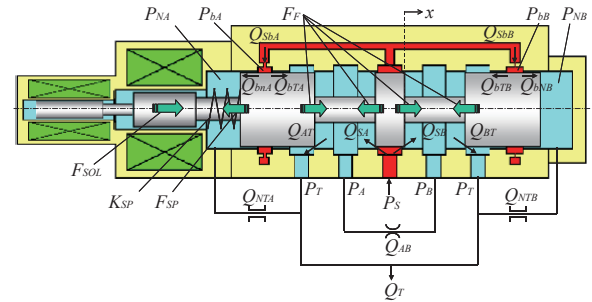Fig. 6 shows the parameter definition diagram for the analysis model.
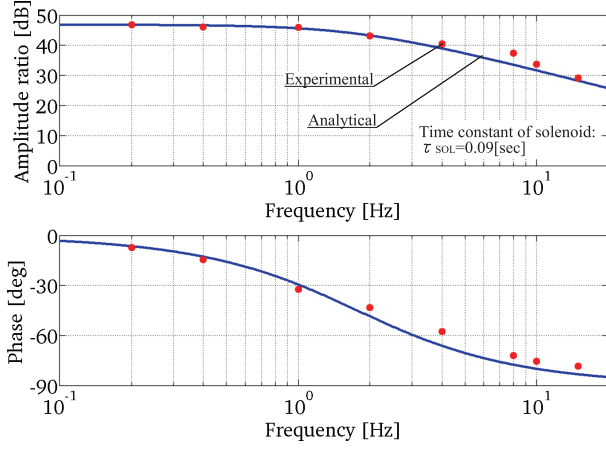

Fig. 6 Parameter definition

As previously mentioned, this valve can be considered to consist of the 3 elements of the compensation circuit, solenoid, and pilot valve sections. The compensation circuit is defined as formula (1) as a general PI controller.

$$C(s)=k_P\left(1+\frac{1}{T_I s}\right) \tag{1}$$

In the previous report, it was experimentally confirmed that solenoid transfer function $S(s)$ can be approached in a first-order lag standard form, and it is defined with the transfer function in formula (2). Fig. 7 shows the experiment result of the thrust frequency characteristic of the solenoid alone and the analysis result comparison for the transfer function in formula (2).

$$S(s)=\frac{K_{SOL}}{\tau_{SOL}\,s+1} \tag{2}$$

Transfer function $P(s)$ for the pilot valve section can be calculated as the first-order lag system transfer function in formula (3) by performing Laplace transformation on the linearized mathematical models of the pressure/flow volume in each section near the experimental points. Parameters in formula (3) are defined by formulas (4) through (19). C_r in formula (15) is the diameter ratio between the damping orifices and hydrostatic bearing

Fig. 7 Solenoid thrust frequency characteristics

orifice. Since there are 4 hydrostatic bearings located in the circumferential direction of the spool, these are represented by equivalent diameter $D_{b'}$, which is defined in formula (14), as one orifice. The ratio is $C_r = D_N / D_{b'}$. The flow from the hydrostatic bearing orifices was determined as laminar flow based on the Reynolds number R_e calculated from the measured flow volume and the geometrics, and the orifices were modeled in formula (12) as choke orifices. With frictional coefficient λ, which determines the damping force of damping orifices, the Blasius equation was applied due to the turbulent flow, as previously mentioned. It was modeled in formula (19).

Among the 3 elements defined above, the transfer characteristics consisting of the solenoid and pilot valve without a compensation circuit are represented in the second-order lag system in formula (20) as the open loop transfer function $V(s)$, which is in the block diagram in Fig. 8. The damping coefficient ζ, natural frequency ω, and proportionality constant K are defined in formulas (21) through (23). Furthermore, as shown in Fig. 5, the closed loop transfer function $V_{SYS}(s)$ for the feedback control of the valve system, including the compensation circuit, is the third-order lag system shown in formula (24).

$$P(s) = \frac{x(s)}{F_{SOL}(s)} = \frac{K_L}{T_L s + 1} \tag{3}$$

$$T_L = \frac{\Gamma - \xi}{K_{SP} + \beta} \tag{4}$$

$$K_L = \frac{1}{K_{SP} + \beta} \tag{5}$$

$$\Gamma = (L_{bn} + L_{bT}) \frac{2\pi \cdot D_{SPL} \cdot \mu}{\delta} \tag{6}$$

$$\xi = \frac{2A^2_{SPL}}{\alpha \cdot \alpha_{bN}} \tag{7}$$

$$\beta = 8 \cdot C \cdot L_W \cdot (P_S - P_L) \cot(\theta) \tag{8}$$

$$\alpha_N = \frac{\pi^2 2^5 D_b^{\,5}}{16 \rho L_{NT} Q_{NT0} \cdot \lambda} C_r^{\,5} \tag{9}$$

$$\alpha = \frac{\alpha_{bN}}{\alpha_{bN} + \alpha_{bT} - \alpha_b} \frac{\alpha_N}{\alpha_{bN}} - 1 \tag{10}$$

$$\alpha_{bN} = \frac{\pi \cdot D_{SPL} \cdot \delta^3}{12 \cdot \mu \cdot L_{bN}} \tag{11}$$

$$\alpha_b = \frac{\pi \cdot D_b^{\,4}}{32 \cdot \mu \cdot L_b} \tag{12}$$

$$\alpha_{bT} = \frac{\pi \cdot D_{SPL} \cdot \delta^3}{12 \cdot \mu \cdot L_{bT}} \tag{13}$$

$$D'_b = 2D_b \tag{14}$$

$$C_r = \frac{D_N}{D'_b} \tag{15}$$

$$D_N = 2C_r D_b \tag{16}$$

$$w = \frac{4Q_{NT0}}{\pi \cdot 2^2 D_b^{\,2}} \frac{1}{C_r^{\,2}} \tag{17}$$

$$\lambda = 0.3164 \cdot \left(2\frac{wD_b}{\nu}\right)^{-0.25} C_r^{\,-0.25} \tag{18}$$
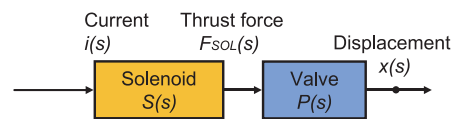
$$R_e = \frac{2wD_b}{\nu} C_r \tag{19}$$

$$V(s) = \frac{K\omega^2}{s^2 + 2\zeta\omega s + \omega^2} \tag{20}$$

$$\omega = \sqrt{\frac{1}{T_L \cdot \tau_{SOL}}} \tag{21}$$

$$\varsigma = \frac{1}{2}\left(\frac{1}{\tau_{SOL}\,\omega} + \tau_{SOL}\,\omega\right) \tag{22}$$

$$K = \frac{K_{SOL}}{K_{SP} + \beta} \tag{23}$$

$$V_{SYS}(s) = \frac{k_P K\omega^2 \left(s + \frac{1}{T_I}\right)}{s^3 + 2\varsigma\omega s^2 + (1 + k_P K)\omega^2 s + \frac{k_P K\omega^2}{T_I}} \tag{24}$$

Fig. 8 Block diagram for the solenoid and pilot valve without the compensation circuit

4 Result and Consideration

It is important to learn the relationship between the transfer characteristics of the open loop transfer function, which is described in Fig. 8, and the equivalent diameter ratio C_r for the damping orifices and hydrostatic bearing orifices before studying the characteristics of the entire valve.

Below are studies on the relationship between the time constant T_L of the pilot valve section's first-order lag system transfer function $P(s)$ in formula (3) and the damping coefficient ζ of the second-order lag system transfer function $V(s)$ of the solenoid and pilot valve section in formula (20) in relation to the changes of C_r, which is defined with the equivalent throttle diameter ratio of the damping orifices and hydrostatic bearing orifices. Fig. 8 shows the relationship between C_r, damping coefficient ζ, and time constant T_L.

4.1 Impact of C_r on Transfer Function $P(s)$ in the Pilot Valve Section

When $C_r > 1$, it means that the damping orifice diameter is relatively larger than the hydrostatic bearing orifice diameter. On the other hand, when $C_r < 1$, it means that the diameter is relatively smaller than the hydrostatic bearing orifice diameter.

Based on the above, the following can be said regarding the relationship between the pilot valve section's transfer function time constant T_L and C_r:

① The smaller C_r is, the larger the time constant T_L value is, delaying the pilot valve section response. This means that the damping orifices have a meter-out effect on the spool operation.

② The larger C_r is, the smaller the time constant T_L value is, accelerating the pilot valve section response. This means that the meter-in effect of the hydrostatic bearing orifices is larger than the meter-out effect of the damping orifices.

③ The overall trend is that time constant T_L inversely decreases against the increase of C_r. The meter-out effect against spool operation also rapidly decreases, and we can say that the effects of damping orifices are almost nonexistent when $C_r > 1.2$.
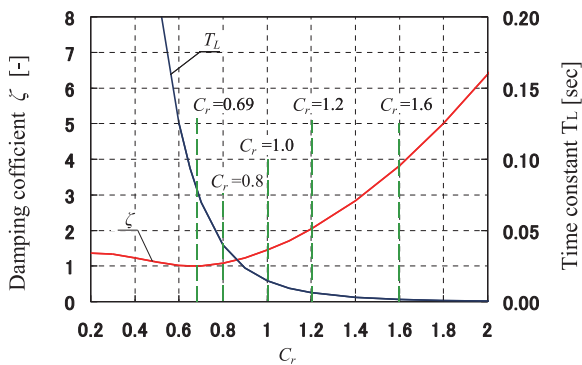
4.2 Impact of C_r on Transfer Function $V(s)$ Represented by the Product of the Pilot Valve Section and the Solenoid

In the same manner, the below can be said regarding the relationship between the C_r and the damping coefficient ζ of the open loop transfer function $V(s)$ represented by the product of the pilot valve section and the solenoid in formula (4) in Fig. 9:

① Regardless of the C_r value, it is always positive. Therefore, in principle, the transfer characteristics of the solenoid and the pilot valve section excluding the compensation circuit are stable.

② When $C_r = 0.69$, the damping coefficient ζ becomes the minimum value of 1. The response critical damping prevents overshoots in the transient response.

③ When $\zeta > 1$, it leads to overdamping, delaying the response.

④ Damping coefficient ζ exponentially increases along with C_r increase, accelerating overdamping.

4.3 Impact of C_r on the Open Loop Transfer Function's Step Response Characteristics excluding the Compensation Circuit

Fig. 10 shows the impact of C_r on the open loop transfer function's step response characteristics. This is when C_r is between 0.69 and 1.6.

The smaller the C_r is, the larger the time constant T_L of transfer function $P(s)$ becomes, indicating the trend to accelerate the rise.

The larger the C_r is, the smaller the time constant T_L of transfer function $P(s)$ becomes, accelerating the rise. However, increased damping coefficient ζ of transfer function $V(s)$ causes overdamping, which means that this is not necessarily a good response. When C_r is 1 or greater, not much difference in the stabilization time is observed.

Due to the above relationship, the pilot valve section response is delayed due to the meter-out effect of the damping orifices when C_r is small, and the response is delayed due to overdamping caused by the increased damping coefficient ζ when C_r is large. Due to this, it is considered that the appropriate value for C_r is between 0.69 and 1.6.

Fig. 9 Relationship between C_r, damping coefficient ζ, and time constant T_L
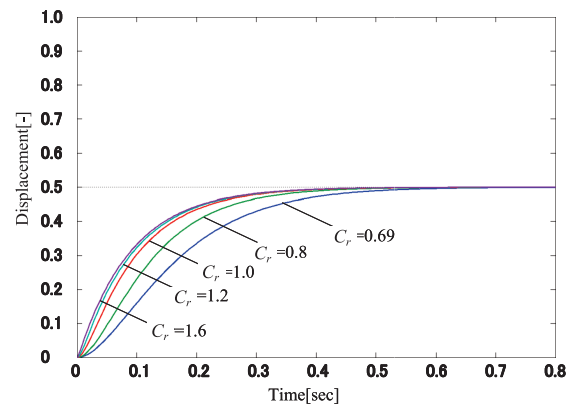

Fig. 10 Impact of C_r on the open loop transfer function's step response characteristics

4.4 Impact of C_r on the Valve's Overall Step Response Characteristics

The above result indicated that there is an appropriate range for C_r. It also indicated that the transfer characteristics, which are calculated from the solenoid's thrust property and the geometric construction of the pilot valve section, are always stable. This section considers the entire valve's response characteristics, including the compensation circuit.

This valve generally composes a feedback control system including a compensation circuit, and the closed loop transfer function indicates third-order transfer characteristics, according to formula (25).

Fig. 11 shows the impact of C_r on the step response of the closed loop transfer function. Based on this result, the compensation circuit's impact is studied from the perspective of step response characteristics of this valve. In this study, C_r is between 0.69 and 1.6, the proportional gain K_P of the compensation circuit is 1.9, and the integral time T_I is 0.1sec. When C_r is 0.69, the rise is slow with damped oscillation and slow convergence. The trend shows that as C_r grows from 0.69 to 1, the rise as well as the convergence accelerate. Furthermore, when comparing C_r 1.2 and 1.6, the rise is faster with $C_r = 1.6$ but it rapidly attenuates. The stabilization time is longer than that of $C_r = 1.2$. It is assumed that the fast rise is largely affected by the time constant T_L, and the damping effect rapidly functions after the point of inflection as it reaches the target, due to the effect of damping coefficient ζ.

In the same manner, Fig. 12 and Fig. 13 show the impact of C_r with different proportional gain and integral time. However, the proportional gain K_P is 4 and the integral time T_I is 0.1sec in Fig. 12, and the proportional gain K_P is 1.9 and the integral time T_I is 0.05 in Fig. 13. These results show that the smaller the C_r is, the slower the rise is, regardless of the proportional gain and integral time, and it comes to convergence with damped oscillation. The trend shows that when the C_r is too large, the rise is fast, but the stabilization time is prolonged.

In general, the faster the rise is, the more likely overshoots are to occur. However, this trend is not observed with this valve. As Fig. 10 indicated, the rise speed is due to the time constant T_L of the pilot valve section's transfer function $P(s)$, and the property while the value is approaching the steady-state value until convergence is due to the damping coefficient ζ of transfer function $V(s)$, combining the solenoid and pilot valve section.

Due to the above result and the perspectives of rise speed and damping force, etc., it is considered that the appropriate value for C_r is between 0.69 and 1.6. The proportional gain and the integral time for the compensation circuit should be determined from both aspects of valve safety and response, and the appropriate value needs to be set within a certain range.
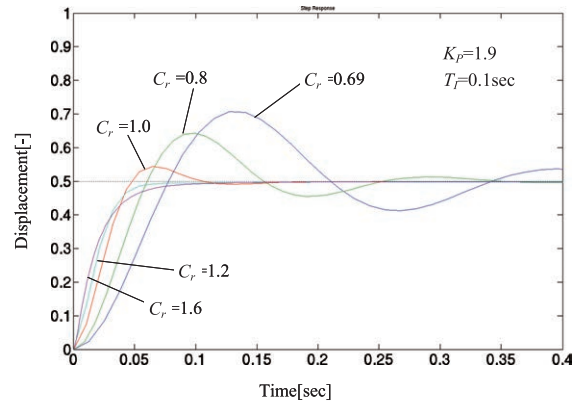

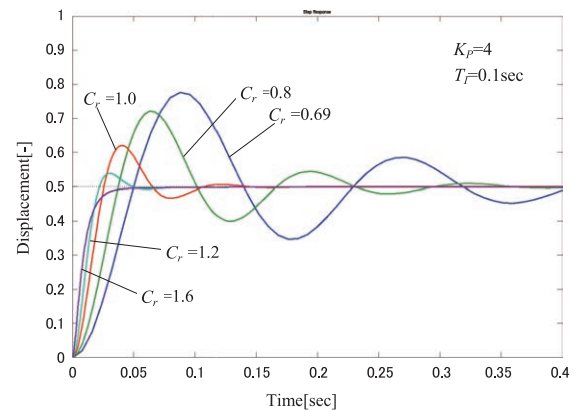**Fig. 11** Impact of C_r on the step response characteristics ($K_P = 1.9$, $T_I = 0.1$sec)

Fig. 12 Impact of C_r on the step response characteristics ($K_P = 4$, $T_I = 0.1$sec)
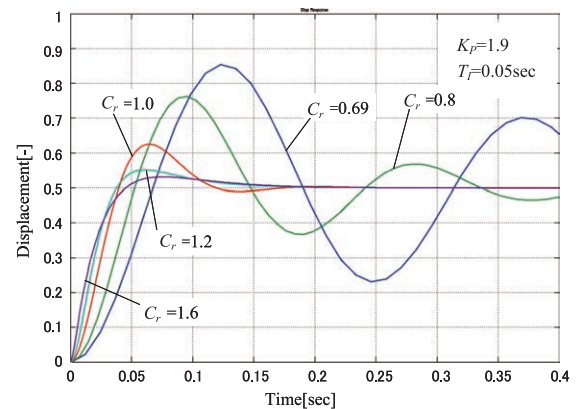

Fig. 13 Impact of C_r on the step response characteristics ($K_P = 1.9$, $T_I = 0.05$sec)

5　Experimental Verification

The analytical verification up to the previous chapter has clarified that C_r is optimal when between 0.69 and 1.6 based on the quick step response launch characteristic, damping characteristic, etc. This was experimentally verified.

5.1 Experiment Method

Fig. 14 shows the summary of the experiment device

for the step response characteristics. The procedure was as follows: The valve's neutral point is adjusted with the stop valve closed. While inputting 50% input signal to the controller as the equilibrium point in the experiment, the load pressure difference P_L between ports A and B is adjusted to 7MPa while opening the stop valve. After adjusting the load pressure, the input signal is switched to 0. The input signal is input to the valve as a step waveform of 0 -> 50%. The input signal u and spool displacement x are recorded by the measuring instrument in chronological order. The provided pressure Ps is 14MPa, and water temperature is 25 +/- 5˚C.
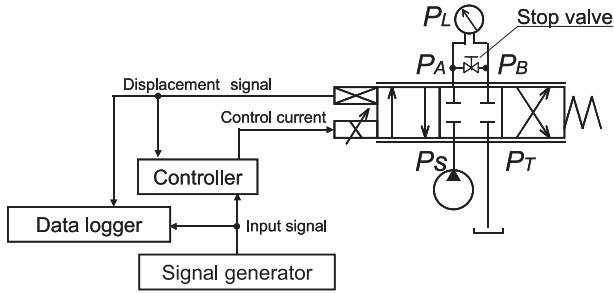

Fig. 14 Summary of the experiment device for the step response characteristics

5.2 Experiment Result

Fig. 15 shows an example of the experiment result for the effect of C_r on the step response characteristics. However, the compensation circuit parameter was adjusted to further clearly demonstrate the effect of C_r, and the spool displacement was normalized by excluding the stationary error. When C_r is 0.9, it proportionally rises in approximately 50m sec before reaching the steady-state value. When C_r is 2, the rise is faster than when C_r is 0.9, but the slope reduces after the point of inflection when it reaches approximately 95% of the target before reaching the target. This is assumed to be caused by the fast rise when C_r is large due to the small time constant T_L as well as the overdamping effect from the large damping coefficient following this point of inflection. This result indicated the same tendency as the analysis result that the rise is slow when C_r is small and that the rise is fast when C_r is large, but the stabilization time is increased due to the overdamping effect.
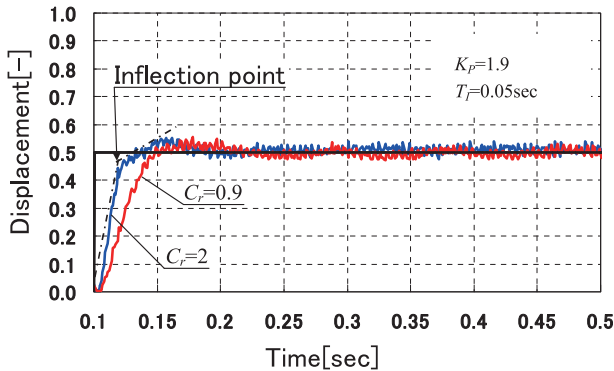

Fig. 15 Experiment result for the effect of C_r on the step response characteristics(K_P=1.9, T_I=0.05sec)

6 Concluding Remarks

① When C_r is small, the pilot valve section response is delayed due to the meter-out effect of the damping orifices. When C_r is large, the response is delayed due to the overdamping caused by the increased damping coefficient ζ. Due to this, the appropriate value of C_r is between 0.69 and 1.6.

② In terms of step response characteristics, the convergence until the target value is slow due to the slow rise when C_r is too small. On the other hand, when C_r is too large, the rise will be fast, but it leads to overdamping; the convergence until the target value is delayed. The result showed the tendency that the rise is fast and the convergence is also fast when C_r is within a certain range.

③ The findings above were also clarified in the experiment result.

Symbol

Designation	Denotation	Unit
A_{SPL}	Spool Cross-sectional area	[m^2]
D'_b	Equivalent orifice diameter	[Pa]
D_{SPL}	Spool diameter	[m]
D_n	Damping orifice diameter	[m]
F_F	Flow force	[N]
F_{SOL}	Solenoid thrust	[N]
K_{SP}	Spring constant	[N/m]
K_{SOL}	Constant of solenoid thrust	[N/A]
L_W	Control orifice width	[m]
$L_{bn}, L_{bT} L_{NT}$	Annular clearance lengh	[m]
P	Supply pressure	[Pa]
Q	Flow rate	[m^3/s]
ζ	Damping coefficient	[–]
λ	Friction facter	[–]
θ	Jet angle	[degree]
δ	Radial clearance	[m]
μ	Viscosity	[Pa s]
v	Kinetic viscosity	[m^2/s]
ρ	Working fluid density	[kg/m^3]
k_P	Proportional gain	[–]
T_I	Integral time	[sec]
τ_{SOL}	Time constant	[sec]
β	Coefficient of flow force	[N/m]
Γ	Coefficient of viscosity	[Ns/m]
C	Flow constant	[–]
C_r	Ratio of orifice diameter	[–]

References

1) Miyakawa, S., Yamashina, C., Takahashi, T.: Development of Water Hydraulic Proportional Control Valve, the Fourth JHPS International Symposium on Fluid Power, ISBN4-931070-04-3.

2) "Development of Water Hydraulic Proportional Valves", YOSHIDA Futoshi, MIYAKAWA Shimpei, KYB TECHNICAL REVIEW No. 42 pp. 3-9 (April, 2011)

3) Yoshida, F., Miyakawa, S.: Characteristics of Proportional Control Valve Using Tap Water, Proceedings of the 7th International Fluid Power Conference, Group H, 445-456, (2010), Aachen, Germany.

3) Yoshida, F., Miyakawa, S.: Dynamic Characteristics of Proportional Control Valve Using Tap Water - Experimental Examination-, Proceedings of the Twelfth Scandinavian International, Conference on Fluid Power, Vol.2 pp. 469-480, (2011), Tampere, Finland.

4) Yoshida, F., Miyakawa, S.: Effect of Parameters on Frequency Characteristics of Proportional Control Valve Using Tap Water, Proceedings of the 8th JFPS international Symposium on Fluid Power in Okinawa, Japan, on October 25-28, (2011), CD-ROM.

5) YOSHIDA Futoshi, "Development and Application of Water Hydraulic Proportional Control Valves", KYB TECHNICAL REVIEW No. 48 pp. 17-23 (April, 2014)

6) Yoshida, F., Miyakawa, S.: Effect of Design Parameter on Response Characteristics of Water hydraulic proportional Control Valves, Proceedings of the 13th Scandinavian International Conference on Fluid Power, (2013), Linkoping, Sweden.

─── **Author** ───

YOSHIDA Futoshi

Joined the company in 1998.
Staff Manager, New Business Development Dept. (stationed at Sagami Plant), Engineering Div.
Engaged in research and development of hydraulic equipment/ systems.